Supplement of Atmos. Chem. Phys., 22, 3945–3965, 2022
https://doi.org/10.5194/acp-22-3945-2022-supplement


Atmospheric Chemistry and Physics
Open Access
EGU

*Supplement of*

# Reducing future air-pollution-related premature mortality over Europe by mitigating emissions from the energy sector: assessing an 80 % renewable energies scenario

**Patricia Tarín-Carrasco et al.**

*Correspondence to:* Pedro Jiménez-Guerrero (pedro.jimenezguerrero@um.es)

## Target domain

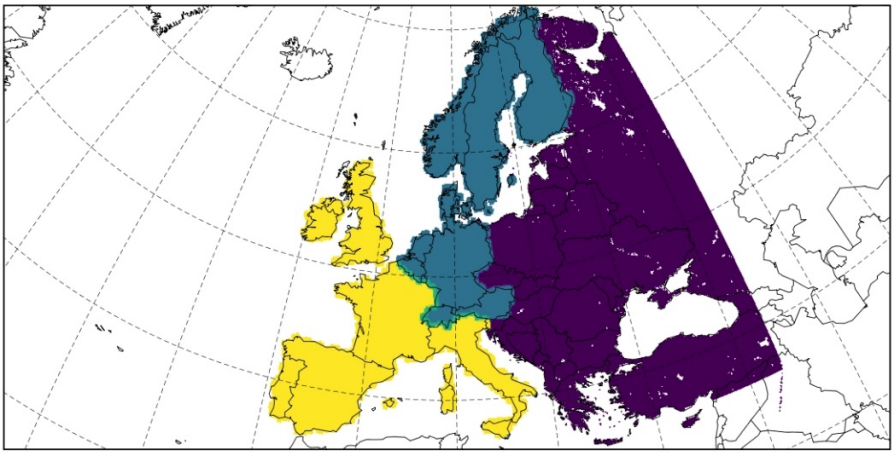

**Figure S1.** Target domain and European regions included in this contribution: Western Europe (yellow), Central Europe (blue) and Eastern Europe (purple).

**Population density**

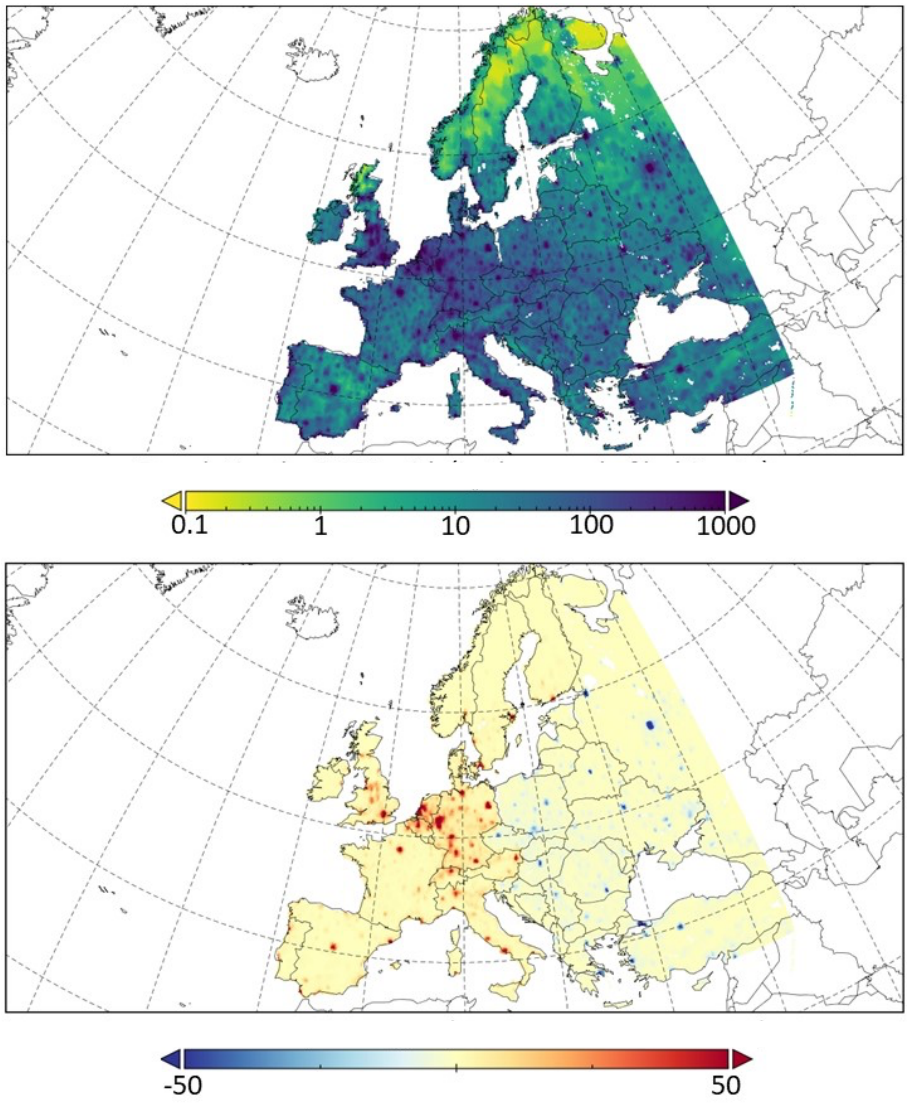


**Figure S2.** Population density (pop/km$^2$) in each grid cell for the present case (top) and difference with UN-projected population in 2050 (bottom) over the European target domain (pop/km$^2$).

## WRF-Chem physico-chemical configuration used in the simulations

**Table S1.** WRF-Chem physico-chemical configuration used in the simulations.

| Scheme | Option | Reference |
|---|---|---|
| **Physics** | | |
| Microphysics | Lin | Lin et al. (1983) |
| SW & LW radiation | RRTM | Iacono et al. (2008) |
| Planetary boundary layer | YSU | Hong et al. (2006) |
| Cumulus | Grell 3D | Grell and Dévényi (2002) |
| Soil | Noah | Tewari et al. (2004) |
| **Chemistry** | | |
| Gas-phase | RACM-KPP | Stockwell et al. (1997) |
| | | Geiger et al. (2003) |
| Aerosols | GOCART | Ginoux et al. (2001) |
| | | Chin et al. (2002) |
| Photolysis | Fast-J | Fast et al. (2006) |
| Biogenic emissions | MEGAN | Guenther et al. (2006) |
| Anthropogenic emissions | ACCMIP | Lamarque et al. (2010) |

**Model evaluation of PM2.5 concentrations against available concentrations**

In this Section we compare the WRF-Chem output for PM2.5 with available data. Hence, the modelling results for fine particulate matter were validated against data from 108 AirBase air quality stations (Figure 3,a from the European Environment Agency, data publicly available through https://discomap.eea.europa.eu/App/AirQualityStatistics/index.html#) for Europe during the years 1991 and 2010. The station data fulfilled a double condition: (1) stations were background stations, so the spatial coverage of the station fits the working resolution of the model; and (2) the availability of data at the station was higher than 50% for the target period.

Statistical metrics used in this evaluation have been widely used in previous works regarding validation of air quality models (e.g. Ratola and Jiménez-Guerrero (2016); Nopmongcol et al. (2017); Odman et al. (2020); among many others) and cover the mean values of model and observations 3,b and c, respectively), bias metrics (mean bias, B; mean fractional bias, MFB) and error metrics (root mean square error, RMSE; mean fractional error, MFE). These statistics and errors are defined and summarized in Table SM2. Table SM3 presents the evaluation results for each individual station included in this contribution.

**Table S2.** Summary of statistical figures used for PM2.5 validation, where $c$ is the concentration of the model ($m$) or the observations ($o$). $c_{mm}$ and $c_{om}$ represent the mean concentrations of the model and the observations, respectively.

| **Parameter** | **Definition** | **Value** |
|---|---|---|
| Mean Bias (B) | $B = \frac{1}{N}\sum(c_m - c_o)$ | 1.94 $\mu$g m$^{-3}$ |
| Root Mean Square Error (RMSE) | $RMSE = \sqrt{\frac{\sum(c_m - c_o)^2}{N}}$ | 3.75 $\mu$g m$^{-3}$ |
| Mean Fractional Bias (MFB) | $MFB = \frac{1}{N}\sum \frac{(c_m - c_o)}{\frac{(c_m + c_o)}{2}}$ | 8.95% |
| Mean Fractional Error (MFE) | $MFE = \frac{1}{N}\sum \frac{\lvert c_m - c_o \rvert}{\frac{(c_m + c_o)}{2}}$ | 27.50% |

**Table S3.** Summary of statistical figures for each station, according to the statistical parameters defined in Table 2.

| Station | EoI Code | Longitude | Latitude | Mod. ($\mu$g m$^{-3}$) | Meas. ($\mu$g m$^{-3}$) | B ($\mu$g m$^{-3}$) | MFB (%) | MFE (%) | RMSE ($\mu$g m$^{-3}$) |
|---|---|---|---|---|---|---|---|---|---|
| 1 | AT4S108 | 14.5747 | 48.5311 | 10.91 | 11.06 | -0.15 | -1.24 | 1.37 | 0.17 |
| 2 | AT30302 | 16.6753 | 48.0503 | 15.23 | 13.44 | 1.79 | 11.25 | 12.50 | 1.97 |
| 3 | AT0ILL1 | 16.7664 | 47.7703 | 19.17 | 13.08 | 6.08 | 33.95 | 37.73 | 6.69 |
| 4 | BETN029 | 2.5823 | 51.0163 | 17.47 | 12.06 | 5.41 | 32.95 | 36.62 | 5.95 |
| 5 | BETR833 | 4.3610 | 51.3282 | 17.99 | 13.18 | 4.80 | 27.74 | 30.82 | 5.28 |
| 6 | BETN085 | 6.0017 | 50.3032 | 10.17 | 11.72 | -1.55 | -12.78 | 14.20 | 1.71 |
| 7 | BETN063 | 4.6683 | 50.6554 | 15.21 | 12.66 | 2.56 | 16.50 | 18.33 | 2.81 |
| 8 | BEGRT01 | 5.0533 | 51.2309 | 17.79 | 13.47 | 4.31 | 24.84 | 27.61 | 4.75 |
| 9 | BETN100 | 4.5948 | 50.0957 | 11.20 | 12.16 | -0.96 | -7.36 | 8.18 | 1.05 |
| 10 | BETN093 | 5.2352 | 50.2745 | 12.67 | 11.88 | 0.79 | 5.79 | 6.43 | 0.87 |
| 11 | BETN132 | 5.6304 | 49.7193 | 11.80 | 11.93 | -0.13 | -1.00 | 1.11 | 0.14 |
| 12 | BG0070A | 23.2439 | 42.6372 | 8.99 | 12.76 | -3.77 | -31.22 | 34.69 | 4.15 |
| 13 | BG0053R | 24.7381 | 41.6943 | 7.34 | 11.14 | -3.80 | -37.03 | 41.15 | 4.18 |
| 14 | CY0002R | 33.0578 | 35.0380 | 15.71 | 11.15 | 4.56 | 30.59 | 33.99 | 5.02 |
| 15 | CZ0ESVR | 16.0342 | 49.7351 | 10.94 | 13.12 | -2.18 | -16.28 | 18.09 | 2.39 |
| 16 | CZ0UDOK | 14.1702 | 50.4589 | 21.52 | 12.88 | 8.64 | 45.22 | 50.24 | 9.50 |
| 17 | CZ0ULOM | 13.6734 | 50.5858 | 21.10 | 11.88 | 9.22 | 50.30 | 55.89 | 10.14 |
| 18 | CZ0BMIS | 16.7245 | 48.7918 | 19.91 | 13.95 | 5.96 | 31.66 | 35.18 | 6.55 |
| 19 | EE0011R | 25.9306 | 59.4944 | 6.09 | 9.40 | -3.31 | -38.48 | 42.75 | 3.64 |
| 20 | EE0009R | 26.7589 | 58.7028 | 6.89 | 10.53 | -3.64 | -37.65 | 41.83 | 4.01 |
| 21 | FI00349 | 24.6849 | 60.3144 | 8.19 | 10.31 | -2.12 | -20.64 | 22.93 | 2.33 |
| 22 | FI00208 | 27.6714 | 60.5261 | 8.70 | 10.30 | -1.61 | -15.23 | 16.92 | 1.77 |
| 23 | FI00351 | -0.4583 | 48.6450 | 11.60 | 9.43 | 2.16 | 18.50 | 20.56 | 2.38 |
| 24 | FR21050 | 4.6300 | 49.9078 | 18.63 | 12.19 | 6.44 | 37.60 | 41.78 | 7.08 |
| 25 | FR14008 | 2.6101 | 46.8147 | 12.61 | 9.55 | 3.06 | 24.86 | 27.62 | 3.37 |
| 26 | FR34038 | 0.1797 | 43.6303 | 13.51 | 8.47 | 5.04 | 41.26 | 45.85 | 5.54 |
| 27 | FR12020 | -0.7437 | 46.6567 | 14.99 | 9.33 | 5.66 | 41.89 | 46.54 | 6.23 |
| 28 | FR23124 | 5.7856 | 49.0658 | 20.96 | 14.96 | 6.01 | 30.10 | 33.44 | 6.61 |
| 29 | FR30033 | 7.9080 | 47.9133 | 8.15 | 12.01 | -3.87 | -34.54 | 38.38 | 4.26 |
| 30 | DEUB004 | 7.7645 | 47.8099 | 7.44 | 11.95 | -4.51 | -41.83 | 46.48 | 4.96 |
| 31 | DEBW031 | 10.7567 | 52.8008 | 15.07 | 10.97 | 4.09 | 28.29 | 31.44 | 4.50 |
| 32 | DEUB005 | 10.2406 | 54.0932 | 16.21 | 10.09 | 6.12 | 41.87 | 46.53 | 6.73 |
| 33 | DESH008 | 11.0434 | 51.6624 | 14.97 | 11.06 | 3.91 | 27.03 | 30.03 | 4.30 |
| 34 | DEST098 | 8.1481 | 51.5707 | 17.34 | 12.43 | 4.90 | 29.65 | 32.94 | 5.39 |
| 35 | DENW068 | 7.7299 | 50.4243 | 10.30 | 11.84 | -1.54 | -12.53 | 13.92 | 1.69 |
| 36 | DERP028 | 11.8914 | 51.8373 | 20.41 | 13.05 | 7.36 | 39.59 | 43.98 | 8.10 |
| 37 | DEST104 | 10.6125 | 51.7582 | 6.34 | 8.16 | -1.82 | -22.59 | 25.10 | 2.00 |
| 38 | DENI051 | 7.8265 | 49.2703 | 9.13 | 13.49 | -4.36 | -34.70 | 38.56 | 4.80 |
| 39 | DERP017 | 13.0094 | 51.3038 | 13.69 | 11.46 | 2.22 | 15.91 | 17.67 | 2.44 |
| 40 | DESN076 | 11.1671 | 52.9570 | 12.99 | 10.70 | 2.29 | 17.42 | 19.35 | 2.52 |
| 41 | DENI031 | 8.9282 | 51.4309 | 13.36 | 11.61 | 1.75 | 12.63 | 14.03 | 1.93 |
| 42 | DEHE046 | 14.0153 | 52.5638 | 21.03 | 11.97 | 9.06 | 49.43 | 54.92 | 9.97 |
| 43 | DEBB053 | 14.0153 | 52.5638 | 21.03 | 11.97 | 9.06 | 49.43 | 54.92 | 9.97 |
| 44 | DEBB053 | 12.9619 | 42.5725 | 7.71 | 9.79 | -2.08 | -21.36 | 23.73 | 2.28 |
| 45 | IT0989A | 13.3367 | 42.9006 | 5.73 | 8.03 | -2.30 | -30.11 | 33.46 | 2.53 |
| 46 | IT1842A | 12.3342 | 44.9508 | 16.47 | 12.55 | 3.92 | 24.29 | 26.99 | 4.31 |
| 47 | IT1212A | 11.4333 | 46.5892 | 8.28 | 9.41 | -1.12 | -11.44 | 12.72 | 1.24 |
| 48 | IT0505A | 12.9522 | 43.4681 | 9.35 | 10.96 | -1.62 | -14.33 | 15.92 | 1.78 |
| 49 | IT1773A | 13.6747 | 43.3356 | 11.67 | 10.99 | 0.69 | 5.44 | 6.05 | 0.75 |
| 50 | IT1796A | 11.0708 | 44.9969 | 23.68 | 16.09 | 7.59 | 34.33 | 38.15 | 8.34 |
| 51 | IT1865A | 8.9150 | 45.0408 | 18.58 | 13.54 | 5.04 | 28.27 | 31.41 | 5.55 |
| 52 | IT1736A | 8.3103 | 44.8080 | 20.75 | 21.10 | -0.34 | -1.48 | 1.64 | 0.38 |
| 53 | IT1948A | 10.6639 | 44.8731 | 24.05 | 16.60 | 7.45 | 32.98 | 36.65 | 8.19 |
| 54 | IT1914A | 11.1780 | 44.9278 | 22.06 | 14.03 | 8.02 | 40.02 | 44.47 | 8.83 |
| 55 | IT1921A | 11.6394 | 44.6622 | 21.01 | 13.48 | 7.53 | 39.32 | 43.69 | 8.29 |
| 56 | IT1451A | 12.6275 | 43.9328 | 15.00 | 11.43 | 3.57 | 24.31 | 27.02 | 3.93 |
| 57 | IT1464A | 10.0192 | 44.9894 | 21.91 | 13.33 | 8.58 | 43.85 | 48.72 | 9.44 |
| 58 | IT1924A | 10.2889 | 44.6575 | 15.64 | 12.21 | 3.42 | 22.13 | 24.59 | 3.77 |
| 59 | IT1911A | 11.1144 | 46.1969 | 15.12 | 10.64 | 4.47 | 31.25 | 34.72 | 4.92 |
| 60 | IT1930A | 13.6744 | 41.6700 | 15.24 | 10.36 | 4.88 | 34.32 | 38.14 | 5.37 |

**Table S3.** (continued)

| Station | EoI Code | Longitude | Latitude | Mod. | Meas. | B | MFB (%) | MFE (%) | RMSE |
|---|---|---|---|---|---|---|---|---|---|
| 61 | IT0992A | 12.0617 | 44.1303 | 16.54 | 11.83 | 4.71 | 29.90 | 33.22 | 5.18 |
| 62 | IT1909A | 11.9422 | 44.7417 | 19.35 | 13.02 | 6.33 | 35.20 | 39.11 | 6.96 |
| 63 | IT1927A | 21.1733 | 56.1623 | 11.95 | 9.78 | 2.17 | 17.96 | 19.96 | 2.39 |
| 64 | LV0010R | 25.9056 | 57.1349 | 10.49 | 11.19 | -0.71 | -5.87 | 6.53 | 0.78 |
| 65 | LV0016R | 26.0042 | 55.4633 | 9.96 | 10.39 | -0.43 | -3.81 | 4.23 | 0.47 |
| 66 | LT00051 | 5.8471 | 49.7318 | 16.35 | 12.24 | 4.10 | 25.84 | 28.71 | 4.51 |
| 67 | MT00007 | 4.5103 | 52.2981 | 15.18 | 11.94 | 3.24 | 21.54 | 23.93 | 3.57 |
| 68 | NL00444 | 4.9264 | 51.9714 | 17.22 | 12.65 | 4.57 | 27.53 | 30.59 | 5.03 |
| 69 | NL00620 | 5.8536 | 51.5411 | 17.92 | 12.95 | 4.97 | 28.96 | 32.17 | 5.46 |
| 70 | NL00131 | 5.0508 | 52.8047 | 13.80 | 11.14 | 2.66 | 19.23 | 21.37 | 2.93 |
| 71 | NL00538 | 6.2775 | 53.3317 | 13.76 | 10.07 | 3.69 | 27.87 | 30.96 | 4.06 |
| 72 | NL00934 | 4.5139 | 51.6528 | 14.95 | 12.72 | 2.23 | 14.50 | 16.11 | 2.45 |
| 73 | NL00246 | 5.7086 | 52.1125 | 18.59 | 12.61 | 5.98 | 34.48 | 38.32 | 6.57 |
| 74 | NL00738 | 8.2519 | 58.3885 | 3.41 | 5.40 | -1.99 | -40.63 | 45.14 | 2.19 |
| 75 | NO0002R | 19.4588 | 50.7109 | 21.85 | 17.42 | 4.43 | 20.30 | 22.55 | 4.87 |
| 76 | PL0243A | 15.4317 | 51.3176 | 17.47 | 12.61 | 4.86 | 29.07 | 32.30 | 5.34 |
| 77 | PL0505A | 22.0381 | 54.1248 | 15.17 | 12.05 | 3.12 | 20.63 | 22.93 | 3.43 |
| 78 | PL0005R | 17.9340 | 53.6621 | 19.54 | 12.81 | 6.73 | 37.44 | 41.60 | 7.40 |
| 79 | PL0077A | -8.6939 | 41.8022 | 8.31 | 11.53 | -3.23 | -29.26 | 32.51 | 3.55 |
| 80 | PT01047 | -7.3975 | 38.6150 | 9.11 | 7.58 | 1.53 | 16.54 | 18.37 | 1.69 |
| 81 | PT04006 | -7.7908 | 41.3714 | 3.59 | 5.21 | -1.62 | -33.14 | 36.82 | 1.78 |
| 82 | PT07001 | -8.4661 | 39.3525 | 9.20 | 9.01 | 0.19 | 1.87 | 2.08 | 0.21 |
| 83 | PT03096 | -9.2456 | 39.2783 | 6.50 | 11.93 | -5.43 | -53.05 | 58.94 | 5.97 |
| 84 | PT03102 | -8.7986 | 38.0769 | 12.89 | 9.50 | 3.38 | 27.19 | 30.21 | 3.72 |
| 85 | PT04002 | -8.6906 | 38.6356 | 6.76 | 8.91 | -2.15 | -24.71 | 27.45 | 2.37 |
| 86 | PT03099 | -8.8917 | 39.9239 | 11.84 | 10.13 | 1.70 | 13.93 | 15.48 | 1.87 |
| 87 | PT02019 | -7.3019 | 40.2331 | 6.85 | 6.92 | -0.07 | -0.86 | 0.96 | 0.07 |
| 88 | PT02020 | 20.2911 | 49.1528 | 10.22 | 14.45 | -4.23 | -30.87 | 34.30 | 4.65 |
| 89 | SK0004R | 17.8606 | 47.9600 | 18.43 | 14.51 | 3.92 | 21.42 | 23.80 | 4.31 |
| 90 | SK0007R | 14.8581 | 45.5611 | 11.61 | 11.26 | 0.35 | 2.77 | 3.08 | 0.39 |
| 91 | SI0008R | 0.3728 | 40.5547 | 9.58 | 6.71 | 2.88 | 31.79 | 35.33 | 3.16 |
| 92 | ES0009R | -3.1425 | 41.2742 | 5.66 | 6.41 | -0.75 | -11.19 | 12.43 | 0.8 |
| 2 93 | ES0010R | -6.9236 | 38.4728 | 7.64 | 7.52 | 0.12 | 1.43 | 1.59 | 0.13 |
| 94 | ES0011R | 0.7347 | 41.3939 | 7.32 | 7.25 | 0.06 | 0.79 | 0.88 | 0.07 |
| 95 | ES0008R | -4.3506 | 39.5469 | 5.93 | 6.67 | -0.75 | -10.65 | 11.83 | 0.82 |
| 96 | ES0001R | -5.8975 | 41.2389 | 4.86 | 6.21 | -1.35 | -21.97 | 24.41 | 1.49 |
| 97 | ES0013R | -1.1011 | 39.0828 | 5.47 | 7.16 | -1.68 | -24.01 | 26.68 | 1.85 |
| 98 | ES0012R | -0.8319 | 39.7081 | 9.03 | 6.90 | 2.13 | 24.02 | 26.69 | 2.34 |
| 99 | ES1671A | -1.2814 | 39.5586 | 10.45 | 6.73 | 3.72 | 38.97 | 43.30 | 4.09 |
| 100 | ES1670A | -0.1694 | 40.7350 | 8.40 | 6.54 | 1.86 | 22.40 | 24.89 | 2.05 |
| 101 | ES1811A | -4.2752 | 40.2479 | 9.07 | 6.56 | 2.51 | 28.95 | 32.17 | 2.76 |
| 102 | ES1810A | -3.4679 | 40.9090 | 8.91 | 7.46 | 1.45 | 15.91 | 17.67 | 1.59 |
| 103 | ES1802A | 17.3884 | 58.8058 | 5.69 | 7.67 | -1.97 | -26.59 | 29.55 | 2.17 |
| 104 | SE0012R | 18.6313 | 59.8324 | 4.70 | 6.70 | -2.00 | -31.55 | 35.06 | 2.20 |
| 105 | SE0066A | 13.1500 | 56.0281 | 7.19 | 7.34 | -0.15 | -1.87 | 2.08 | 0.17 |
| 106 | GB0617A | -3.2429 | 55.7922 | 4.03 | 6.98 | -2.94 | -48.14 | 53.49 | 3.24 |
| 107 | GB0048R | -1.3253 | 51.5711 | 8.64 | 9.75 | -1.12 | -10.94 | 12.15 | 1.23 |
| 108 | GB0036R | -1.3253 | 51.5711 | 10.29 | 9.75 | 0.53 | 4.77 | 5.30 | 0.58 |

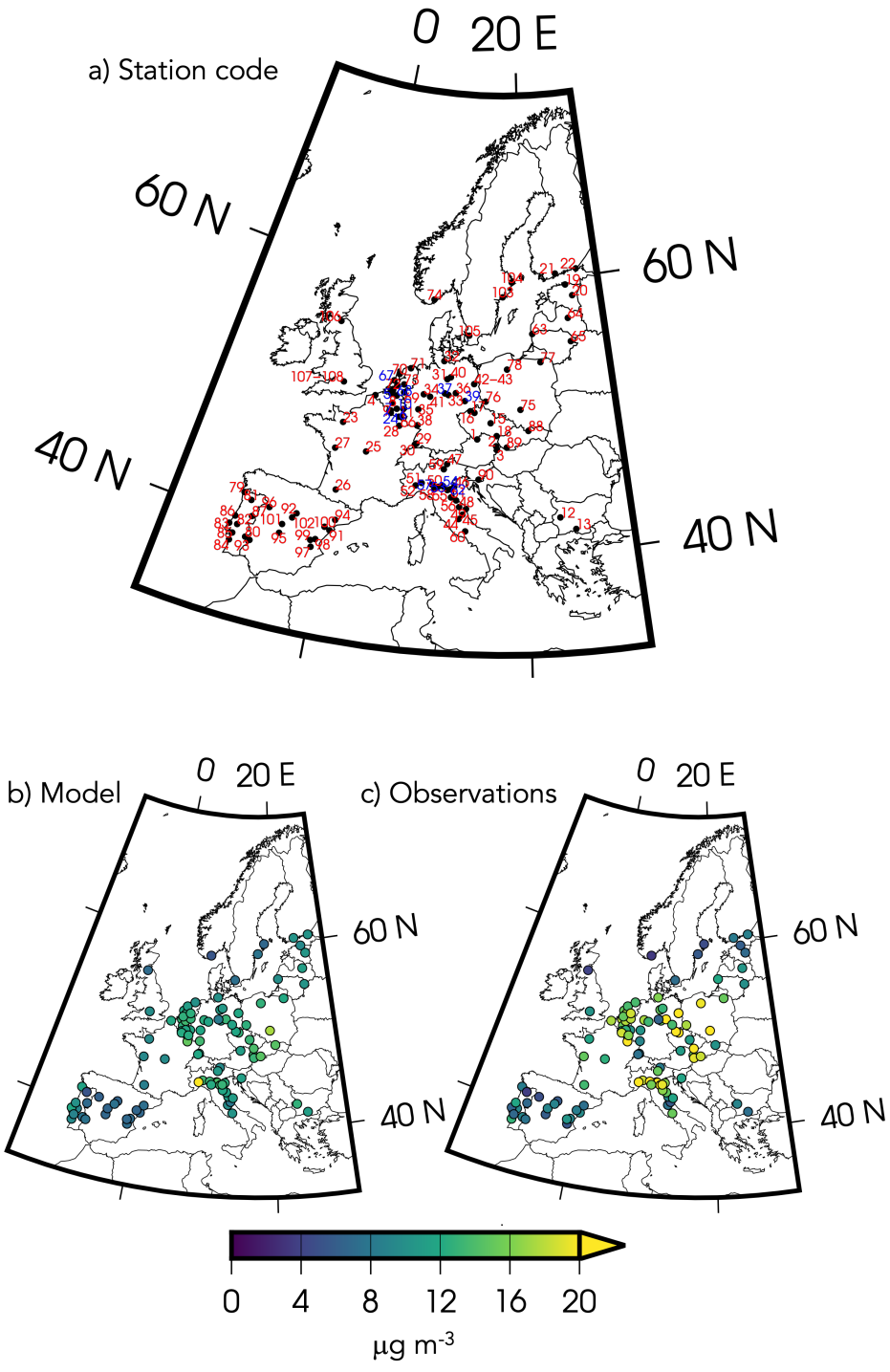


**Figure S3.** (a) Station location and code; (b) Model mean concentration of PM2.5 for 1991-2010; and (c) Observations mean concentration of PM2.5 for 1991-2010.

## Estimated annual premature deaths by age range.

**Table S4.** Estimated annual premature deaths (PD $\times$ $10^3$) by age range in all scenarios covered (in thousands).

| | Present | PRE-P2010 | RCP8.5 | FUT-P2010 | RCP8.5 | REN80-P2010 | RCP8.5 | FUT-P2050 | RCP8.5 | REN80-P2050 |
|---|---|---|---|---|---|---|---|---|---|---|
| Age Range | PD $\times$ $10^3$ | PD/100,000 h. | PD $\times$ $10^3$ | PD/100,000 h. | PD $\times$ $10^3$ | PD/100,000 h. | PD $\times$ $10^3$ | PD/100,000 h. | PD $\times$ $10^3$ | PD/100,000 h. |
| 25-29 | 4.4 | 7.5 | 4.4 | 7.5 | 4.2 | 7.2 | 3.2 | 7.2 | 3.0 | 6.9 |
| 30-34 | 8.0 | 13.8 | 8.0 | 13.8 | 7.7 | 13.3 | 6.4 | 13.6 | 6.2 | 13.0 |
| 35-39 | 12.7 | 22.0 | 12.7 | 22.1 | 12.2 | 21.1 | 10.9 | 22.3 | 10.5 | 21.3 |
| 40-44 | 18.0 | 31.4 | 18.0 | 31.5 | 17.3 | 30.2 | 15.7 | 32.4 | 15.1 | 31.1 |
| 45-49 | 28.5 | 48.0 | 28.5 | 48.1 | 27.4 | 46.2 | 21.8 | 47.6 | 20.9 | 45.7 |
| 50-54 | 43.6 | 77.1 | 43.6 | 77.2 | 41.9 | 74.2 | 34.5 | 75.1 | 33.1 | 72.2 |
| 55-59 | 60.8 | 118.3 | 60.8 | 118.5 | 58.5 | 113.9 | 58.4 | 117.5 | 56.2 | 113.0 |
| 60-64 | 80.0 | 182.5 | 80.1 | 182.6 | 77.0 | 175.6 | 103 .4 | 191.0 | 99.3 | 183.4 |
| 65-69 | 80.7 | 236.9 | 80.8 | 237.2 | 77.8 | 228.4 | 126.7 | 243.8 | 121.8 | 234.3 |
| 70-74 | 112.3 | 328.3 | 112.5 | 328.8 | 108.0 | 315.7 | 153.9 | 321.9 | 147.7 | 308.8 |
| 75-79 | 116.8 | 460.9 | 117.0 | 461.8 | 112.4 | 443.5 | 195 .4 | 458.6 | 187.6 | 440.2 |
| 80+ | 328.7 | 1035.3 | 329.4 | 1037.5 | 317.2 | 999.3 | 807 .5 | 1043.7 | 778.0 | 1005.6 |
| TOTAL | 894.3 | 157.5 | 895.8 | 157.8 | 861.5 | 151.8 | 1537.9 | 254.3 | 1479.3 | 244.7 |

(PRE-P2010): PD for the present case; (FUT-P2010): PD for the future scenario with population at 2010 levels; (REN80-P2010): PD for the future mitigation scenario with population at 2010 levels; (FUT-P2050): PD for the future scenario with population projections of UN for 2050; (REN80-P2010): PD for the future mitigation scenario with population at 2010 levels; (REN80-P2050): PD for the future mitigation scenario with population projections of UN for 2050.

## References


Chin, M., Ginoux, P., Kinne, S., Torres, O., Holben, B. N., Duncan, B. N., Martin, R. V., Logan, J. A., Higurashi, A., and Nakajima, T.: Tropospheric aerosol optical thickness from the GOCART model and comparisons with satellite and Sun photometer measurements, Journal of the Atmospheric Sciences, 59, 461 – 483, https://doi.org/10.1175/1520-0469(2002)059<0461:TAOTFT>2.0.CO;2, 2002.

Fast, J. D., Gustafson Jr., W. I., Easter, R. C., Zaveri, R. A., Barnard, J. C., Chapman, E. G., Grell, G. A., and Peckham, S. E.: Evolution of ozone, particulates, and aerosol direct radiative forcing in the vicinity of Houston using a fully coupled meteorology-chemistry-aerosol model, Journal of Geophysical Research: Atmospheres, 111, D21 305, https://doi.org/10.1029/2005JD006721, 2006.

Geiger, H., Barnes, I., Bejan, I., Benter, T., and Spittler, M.: The tropospheric degradation of isoprene: an updated module for the regional atmospheric chemistry mechanism, Atmospheric Environment, 37, 1503 – 1519, https://doi.org/10.1016/S1352-2310(02)01047-6, 2003.

Ginoux, P., Chin, M., Tegen, I., Prospero, J. M., Holben, B., Dubovik, O., and Lin, S.-J.: Sources and distributions of dust aerosols simulated with the GOCART model, Journal of Geophysical Research: Atmospheres, 106, 20 255 – 20 273, https://doi.org/10.1029/2000JD000053, 2001.

Grell, G. A. and Dévényi, D.: A generalized approach to parameterizing convection combining ensemble and data assimilation techniques, Geophysical Research Letters, 29, 38–1–38–4, https://doi.org/10.1029/2002GL015311, 2002.

Guenther, A., Karl, T., Harley, P., Wiedinmyer, C., Palmer, P. I., and Geron, C.: Estimates of global terrestrial isoprene emissions using MEGAN (Model of Emissions of Gases and Aerosols from Nature), Atmospheric Chemistry and Physics, 6, 3181 – 3210, https://doi.org/10.5194/acp-6-3181-2006, 2006.

Hong, S.-Y., Noh, Y., and Dudhia, J.: A New Vertical Diffusion Package with an Explicit Treatment of Entrainment Processes, Monthly Weather Review, 134, 2318 – 2341, https://doi.org/10.1175/MWR3199.1, 2006.

Iacono, M. J., Delamere, J. S., Mlawer, E. J., Shephard, M. W., Clough, S. A., and Collins, W. D.: Radiative forcing by long-lived greenhouse gases: Calculations with the AER radiative transfer models, Journal of Geophysical Research: Atmospheres, 113, D13 103, https://doi.org/10.1029/2008JD009944, 2008.

Lamarque, J.-F., Bond, T. C., Eyring, V., Granier, C., Heil, A., Klimont, Z., Lee, D., Liousse, C., Mieville, A., Owen, B., Schultz, M. G., Shindell, D., Smith, S. J., Stehfest, E., Van Aardenne, J., Cooper, O. R., Kainuma, M., Mahowald, N., McConnell, J. R., Naik, V., Riahi, K., and van Vuuren, D. P.: Historical (1850–2000) gridded anthropogenic and biomass burning emissions of reactive gases and aerosols: methodology and application, Atmospheric Chemistry and Physics, 10, 7017 – 7039, https://doi.org/10.5194/acp-10-7017-2010, 2010.

Lin, Y.-L., Farley, R. D., and Orville, H. D.: Bulk Parameterization of the Snow Field in a Cloud Model, Journal of Climate and Applied Meteorology, 22, 1065–1092, https://doi.org/10.1175/1520-0450(1983)022<1065:BPOTSF>2.0.CO;2, 1983.

Nopmongcol, U., Liu, Z., Stoeckenius, T., and Yarwood, G.: Modeling intercontinental transport of ozone in North America with CAMx for the Air Quality Model Evaluation International Initiative (AQMEII) Phase 3, Atmospheric Chemistry and Physics, 17, 9931–9943, https://doi.org/10.5194/acp-17-9931-2017, https://acp.copernicus.org/articles/17/9931/2017/, 2017.

Odman, M. T., Qin, M., Hu, Y., Russell, A. G., and Boylan, J. W.: Interstate transport of ozone in eastern United States: An analysis of the impact of southeastern states' emissions in 2017, Atmospheric Environment, 236, 117 628, https://doi.org/https://doi.org/10.1016/j.atmosenv.2020.117628, https://www.sciencedirect.com/science/article/pii/S1352231020303617, 2020.

Ratola, N. and Jiménez-Guerrero, P.: Can biomonitors effectively detect airborne benzo[a]pyrene? An evaluation approach using modelling, Atmospheric Chemistry and Physics, 16, 4271–4282, https://doi.org/doi: 10.5194/acp-16-4271-2016, 2016.

Stockwell, W. R., Kirchner, F., Kuhn, M., and Seefeld, S.: A new mechanism for regional atmospheric chemistry modeling, Journal of Geophysical Research: Atmospheres, 102, 25 847 – 25 879, https://doi.org/10.1029/97JD00849, 1997.

Tewari, M., Chen, F., Wang, W., Dudhia, J., LeMone, M., Mitchell, K., Ek, M., Gayno, G., Wegiel, J., and Cuenca, R.: Implementation and verification of the unified NOAH land surface model in the WRF model, in: 20th Conference on weather analysis and forecasting/16th Conference on numerical weather prediction, pp. 11 – 15, 2004.